2019 IEEE 15th International Conference on Automation Science and Engineering (CASE)

Design and Gait Control of a Quadruped Robot with Low-Inertia Legs

Linlin Shang[1,2], Wei Wang[1,2], and Jianqiang Yi[1,2]

Abstract— **This paper presents a novel quadruped robot, "Biodog II", featuring low-inertia legs and coaxial transmission. Each leg has two degrees of freedoms (DOFs) - a knee and hip joint, which are actuated by proximal mounted DC motors, and a compliant ankle joint. Motor power can be transited to active joints efficiently and accurately by means of coaxial transmission. In particular, we employ a tendon-bone co-location structure on the leg to reduce stress and enhance strength. A Hopf oscillator-based Central Pattern Generator (CPG) is responsible for generating locomotion trajectories of different gaits. An embedded controller based on an ARM board is designed to command motors. Locomotion experiments including walk and trot gait test demonstrate the stability and mobility of Biodog II.**

I. Introduction

Legged robots possess superior stability and maneuverability to traverse various terrains. Compared with biped robots, quadruped robots own better stability and greater load capacity. Moreover, quadruped robots have simpler mechanical structure compared with hexapod and octopod robots. Therefore, quadruped robots have a bright prospect in executing tough tasks, such as disaster rescue, industrial detection and material transportation. After Fukushima Daiichi nuclear disaster, a quadruped robot are designed by Toshiba Corporation for disaster assessment at the most damaged parts of the Fukushima Daiichi Nuclear Power Plant [1]. ANYmal has completed inspection and manipulation tasks regularly and automatically on the offshore converter platform and in sewer systems underneath the city [2]. Despite the rapid development of robotics, there are only a handful of quadruped robots that can be applied to practical engineering. One of main challenges for real-world application is the design of quadruped robots.

There have been many research focusing on designing quadruped robots for highly dynamic tasks. To support soldiers, BigDog developed by Boston Dynamics has successfully performed walking, trotting and bounding on rough terrains with big payload [3]. By combing hydraulically and electrically actuated joints, HyQ and its follower HyQ2max can respond quickly to obstacles to avoid falling and achieve highly dynamic running, jumping and hopping [4], [5]. Scarl*ETH* is featured by a series compliant articulated leg and demonstrates fast, efficient, and versatile locomotion. This platform combines precise torque and position control through series elastic actuation [6]. However, actuators of all platforms presented above are mounted on their legs. As a result, the leg systems become rather large and heavy. This configuration limits the mobility and flexibility of legs and causes unnecessary energy waste.

To develop flexible and reliable quadruped robots, many robotic researchers focus on energy-efficient leg design. Paramount examples are the MIT Cheetach [7], [8] and its successors, the MIT Cheetach 2 [9] and the MIT Cheetan 3 [10]. Thanks to the tailored high torque-density motors and low inertia legs, MIT Cheetach performs dynamic running in high speed on flat ground [7]. Through impulse scaling principles, Cheetach 2 is able to autonomously gallop over obstacles and run at a range of speeds [9]. Cheetach 3, possessing greater range of joint motion and an embedded control architecture, performs dynamic locomotion on unexpected terrains [10]. The MIT Cheetach series demonstrate outstanding running and jumping locomotion at particularly high speed, but they require tailored high torque-density motors and mechanical design. Another example is a direct-drive quadruped robot, Minitaur [11], which represents a novel leg design by getting rid of motor reduction such as a chain, bear or belt. This design affords high effective output torque of motors and high-actuation bandwidth [11]. As a result, Minitaur can bound at 1.45 m/s and jump vertically with height of 48 cm. However, this robot is mainly designed for research purposes and in small size.

Inspired by research on energy-efficient leg design [7]-[11], we present a new quadruped robot, "Biodog II", featuring low-inertia legs and coaxial transmission. Biodog II is an evolution of Biodog developed in our lab [12]. Biodog can only move on specific grounds and its energy consumption is high. In this contribution, our goal is to design a robot with simple mechanical structure, which can perform multiple gaits stably and smoothly with low energy consumption. We plan to apply this robot to detection tasks in a power plant in the future.

Biodog II is motivated by biological systems in terms of both mechanical design and locomotion control strategy. To reduce the leg inertia as much as impossible, all motors are placed proximal and there are only two degrees of freedom (DOFs) per leg. The coaxial transmission is designed to transmit motor power to active joints efficiently and accurately. Besides, each leg has a compliant ankle joint to absorb impacts during touchdown. Particularly, the tendon-bone co-location structure is implemented for high strength. The combination of these configuration results in a mammal-like three-segment leg with low inertia. Considering applying the robot to actual engineering, an embedded controller based on an ARM board has been designed to command the motors. In addition, forward and inverse

*This work was supported in part by the National Natural Science Foundation of China under Grant 61375101.

[1]University of Chinese Academy of Sciences, 19 A Yuquan Road, Shijingshan District, Beijing, 100049, China.

[2]Institute of Automation, Chinese Academy of Sciences, 95 Zhongguan-cun East Road, Beijing, 100190, China.

Corresponding author: Wei Wang, (wei.wang@ia.ac.cn)

978-1-7281-0356-3/19/$31.00 ©2019 IEEE

kinematic analysis of the leg are described in detail for further examination of the leg configuration.

The locomotion trajectories of fundamental gaits are generated by a Central Pattern Generator (CPG) modeled as a network of four coupled Hopf oscillators. This controller is constructed by mimicking the rhythmic motion of animals. For vertebrates, rhythmic motions such as breathing, walking and running are controlled by neural networks located in the spinal cord, named CPGs [13]. In robotics, CPGs are often based on coupled oscillators and used for quadruped locomotion control [14].

II. Mechanical Design of Biodog II

This section presents the mechanical design of Biodog II, with the main components depicted in Fig. 1(a). The mechanical configuration of Biodog II is illustrated in Fig. 1(b). Biodog II is composed of four mammal-like legs and a torso. With the size of 0.42 m in length, 0.22 m in width, and 0.35 m in height, Biodog II weighs slightly less than 25 kg.

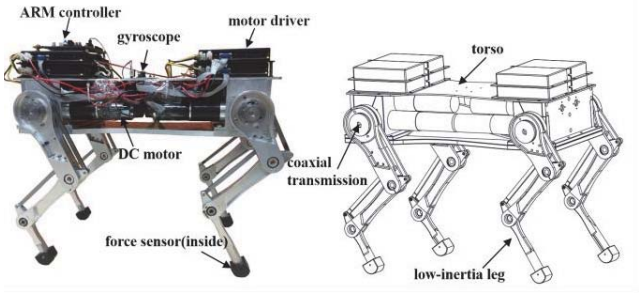

(a) Picture of Biodog II. (b) CAD drawing of Biodog II.

Fig. 1. Picture and CAD drawing of Biodog II.

A. Low-inertia Leg design

The leg design plays a critical role in locomotion performance of quadruped robots. This research proposes a mammal-like leg with three linked rigid mechanical segments that are interconnected with reinforcing bars. To improve flexibility and maneuverability, the inertia of legs has to be reduced as much as possible and the strength of legs needs to be enhanced. We optimize placement of actuators and adopt tendon-bone co-location architecture to fulfill these two goals.

Fig. 2 shows the clarified CAD model of the forelimb module including actuation systems and coaxial transmission. Leg modules of the robot are identical with slight difference in segment length ratios among the three links between fore and rear legs. Each leg has two DOFs, a hip pitch joint and a knee pitch joint. We motivate this choice of two DOFs per leg so as to reduce inertia and simplify the robot structure. Moreover, each leg has a compliant ankle joint to reduce impact force peaks during touchdown. The foot is made from rubber to increase the friction with the ground and prevent the robot from slipping.

The decision of using three leg segments is motivated by biological theory, since mammals have a distinct three-segment limb construction [15], [16]. The leg segments are femur, tibia and metatarsal with successive hip, knee and ankle joint. Tendon-bone co-location leg architecture is implemented for high strength. This design also draws inspiration from mammalian musculoskeletal structures [17], which has already implemented on the MIT Cheetach [8]. The synergetic arrangement of bones and tendons helps reduce the compressive loads when experiencing ground impact [18]. The tendon-bone co-location structure is developed by combination of three links and two reinforcing bars made by high tensile strength alloy, as shown in Fig. 2(b). These reinforcing bars hold these segments together. The reinforcing bar between the femur and tibia segment helps transmit movement from the coaxial transmission to the knee joint. The other one ensures parallelism between the femur and metatarsal segment during locomotion.

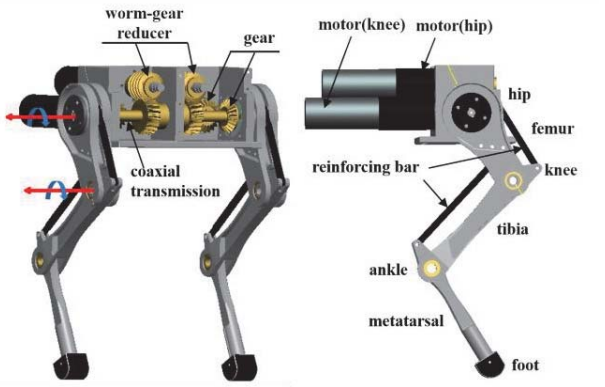

(a) Forelimb (b) RF leg

Fig. 2. Clarified CAD model of forelimb and RF limb.

B. Leg Actuation and Coaxial Transmission

DC motors are suitable for actuating quadruped robots since they have advantage in high torque and efficiency, with low noise. For Biodog II, the hip and knee joint are actuated by two DC motors (150 watt), respectively. Planetary gearheads are equipped with the motors in order to amplify output torque and reduce speed, with reduction of 26:1 for hip joints and 156:1 for knee joints. Besides, each motor is fitted with a precise motor encoder and driven by a positioning controller EPOS2 70/10.

In traditional legged robot design, actuators are usually attached to legs to directly actuate active joints [19]. However, the inertia of legs increases. Therefore, we integrate all motors and coaxial transmission for driving active joints inside the torso, as shown in Fig. 2. Force transmission from motors to hip joints is done by means of the worm-gear reducer with gear ratio of 10:1, while force transmission from motors to knee joints is done by reinforcing bars and gears with gear ratio of 1:1.

C. Control Electrics

Fig. 3 shows the control system layout of Biodog II, which can be roughly divided into four parts: the host computer, the ARM controller, the leg actuation and sensors. The host computer is responsible for modulating the locomotion behavior such as speed and gait. The ARM controller is based on the STM32F103 microprocessor (at 72 MHz), integrated with a serial communication interface (SCI), a Controller Area

Network (CAN) module, three 16-channel A/D converters (ADC), a WIFI module and power-supply module. The function of the ARM controller is not only to perform motion-planning algorithms, but also to acquire and process sensor information. The ARM controller communicates with the host computer through the WIFI module. The control commands calculated by the ARM controller are transferred to motor drivers through CAN bus.

Biodog II is equipped with a gyroscope module and four force sensing resisters (FSRs) so as to apperceive outside environment and its own motion states. As depicted in Fig. 4(a), FSR is responsible for foot-ground contact force detection. When applying force to the active area, FSR exhibits decrease in resistance. As shown in Fig. 4(b) and Fig. 4(c), this force sensor is fixed at the bottom of the metatarsal segment and is sample at 10Hz.

Fig. 4(d) illustrates the gyroscope module, mounted on the upper torso plate. The gyroscope module (at 125Hz), using MPU9250 chip as the core, integrates a 3-axis gyroscope, a 3-axis acceleration sensor and a Digital Motion Processor (DMP). Through this motion tracking device, we can measure the pitch, roll and yaw angles of the robot conveniently.

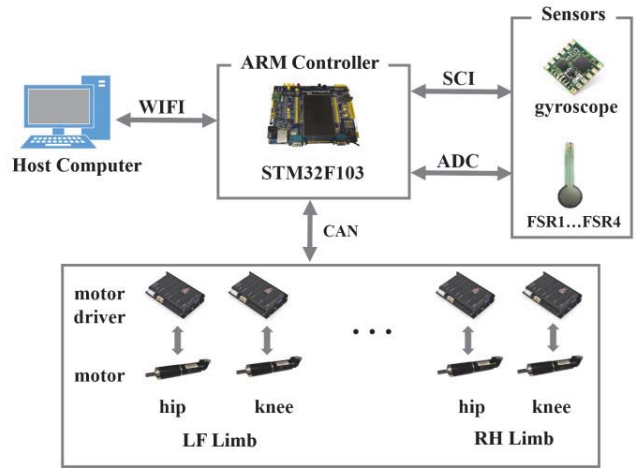

Fig. 3. Overview of the control system architecture (only actuation systems for LF and RH limb are shown here).

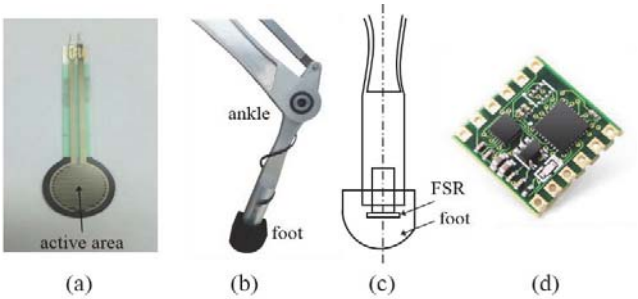

Figure. 4. (a) Force Sensitive Resister (FSR) for detecting foot-ground contact force. (b) Structure of a foot. (c) Structure drawing of a foot and setup of the FSR. (d) Gyroscope module for measuring pitch, roll and yaw angles during locomotion.

III. Forward and Inverse Kinematics Analysis

This section presents forward and inverse kinematic equations of the leg. As an example, development of forward and inverse kinematic equations of the right fore leg is described in detail. Fig. 5 shows the structure of the right fore leg, and a set of coordinate frames are defined to represent the leg configuration.

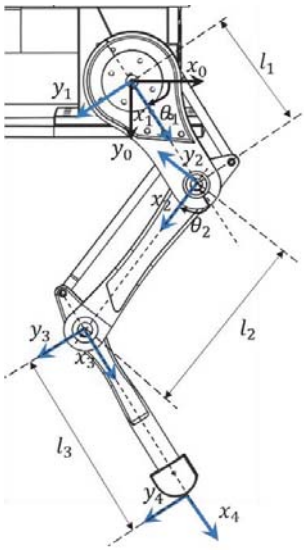

Fig. 5. Configuration model of RF leg and D-H frames {1}, {2}, {3}, {4} defined for kinematics analysis. l_1, l_2 and l_3 represent the length of the femur, tibia and metatarsal segment, respectively.

A. Forward Kinematics

We adopt Denavit-Hartenberg (D-H) method [20] to develop the forward kinematic equations. According to the D-H rules, the D-H frames are established on the leg of Biodog II, as shown in Fig. 5. Coordinate frame {0} is the base frame attached on the torso, and x_0 points the forward direction of the robot, y_0 points opposite to gravity direction. Coordinate frames {1}, {2}, {3} are transitional frames affixed on the hip, knee, ankle joint, separately. In addition, frame {4} affixes itself at the foot. Using D-H transformation matrices, we can calculate the position of the footpad relative to the base frame. The relationship between two adjacent links is expressed as follows:

$$T_1^0 = \begin{bmatrix} \cos\theta_1 & \sin\theta_1 & 0 \\ -\sin\theta_1 & \cos\theta_1 & 0 \\ 0 & 0 & 1 \end{bmatrix}$$

$$T_2^1 = \begin{bmatrix} \cos\theta_2 & \sin\theta_2 & l_1 \\ -\sin\theta_2 & \cos\theta_2 & 0 \\ 0 & 0 & 1 \end{bmatrix} \quad (1)$$

$$T_3^2 = \begin{bmatrix} \cos\theta_2 & -\sin\theta_2 & l_2 \\ \sin\theta_2 & \cos\theta_2 & 0 \\ 0 & 0 & 1 \end{bmatrix}$$

$$T_4^3 = \begin{bmatrix} 1 & 0 & l_3 \\ 0 & 1 & 0 \\ 0 & 0 & 1 \end{bmatrix}$$

where T_i^j represents transformation matrix from the coordinate frame $\{j\}$ to the coordinate frame $\{i\}$. l_1, l_2 and l_3 represent the length of the femur, tibia and metatarsal segment, respectively.

The transformation matrix from frame {4} to frame {0} is obtained as follows:

$$T_4^0 = T_1^0 T_2^1 T_3^2 T_4^3 \tag{2}$$

Multiplying T_4^0 with $(0, 0, 1)^T$, we obtain:

$$\begin{bmatrix} P_x \\ P_y \end{bmatrix} = \begin{bmatrix} l_1 c_1 + l_2 \mathrm{c}_{12} + l_3 (c_2 \mathrm{c}_{12} + s_2 s_{12}) \\ -l_1 s_1 - l_2 s_{12} + l_3 (s_2 \mathrm{c}_{12} - c_2 s_{12}) \end{bmatrix} \tag{3}$$

where $c_1 = \cos(\theta_1)$, $s_1 = \sin(\theta_1)$, $c_2 = \cos(\theta_2)$, $s_2 = \sin(\theta_2)$, $c_{12} = \cos(\theta_1 + \theta_2)$, $s_{12} = \sin(\theta_1 + \theta_2)$.

The vector $(P_x, P_y)^T$ defines the foothold of RF represented in frame{0}. Given the rotation angles of hip and knee joints, we can calculate the locations of the robot footpad relative to the torso through (4). Forward kinematics equations of other legs can be derived as above.

B. Inverse kinematics

Unlike the forward kinematics, multiple solutions may satisfy the inverse kinematics equations simultaneously.

To derive the inverse kinematics equations, we first transform (2) to (5):

$$T_4^1 = (T_1^0)^{-1} T_4^0 \begin{bmatrix} 0 \\ 0 \\ 1 \end{bmatrix} = T_2^1 T_3^2 T_4^3 \begin{bmatrix} 0 \\ 0 \\ 1 \end{bmatrix} \tag{4}$$

Then, we obtain

$$\theta_1 = \mathrm{Atan2}(P_x, -P_y) - \mathrm{Atan2}(d_1, d_2) \tag{5}$$

$$\theta_2 = \mathrm{Atan2}\left[(P_x s_1 - P_y c_1)/(P_x c_1 + P_y s_1 - l_1 - l_3) \right] \tag{6}$$

where

$$d_1 = \left[P_x^2 + P_y^2 + (l_1 + l_3)^2 - l_2^2 \right] / -2(l_1 + l_3) \tag{7}$$

$$d_2 = \pm \sqrt{P_x^2 + P_y^2 - d_1^2} \tag{8}$$

Given the position of the foot with $(p_x, p_y)^T$, we can compute joint angles through (7) and (8).

IV. HOPF OSCILLATOR-BASED CPG FOR LOCOMOTION CONTROL

The locomotion of Biodog II is controlled using a Hopf oscillator-based CPG, inspired by rhythmic motion mechanism of vertebrates in nature. The advantages of this controller are as follows: (a) transient perturbations are promptly forgotten thanks to a globally stable limit cycle, (b) swing and stance durations can be controlled independently, (c) different gaits can be generated by simply modulating the phase relationship between every two oscillators and (d) output signals can be modulated easily by limited parameter change.

The Hopf oscillator is defined by the following equations [21]:

$$\dot{x} = m(\mu - r^2)x - \omega y \tag{9}$$

$$\dot{y} = n(\mu - r^2)y + \omega x \tag{10}$$

$$\omega = \omega_{st} / (e^{-\mathrm{ax}} + 1) + \omega_{sw} / (e^{\mathrm{ax}} + 1) \tag{11}$$

$$r = \sqrt{x^2 + y^2} \tag{12}$$

where μ is the amplitude of oscillations. m and n are positive constants that specify the convergence velocity of state variables x and y, respectively. ω is the frequency, which is determined by two independent parameters: ω_{st}, the frequency of the stance phase and ω_{sw}, the frequency of the swing phase. a is also a positive constant and a=100 in our case.

Quadruped robots normally perform various gaits to adapt to different terrains and keep stability. Four Hopf oscillators are coupled as a CPG network to generate stable rhythmic signals for common gaits, shown as follows [22]:

$$\dot{x}_i = m(\mu - r_i^2)x_i - \omega_i y_i + R_x(\phi_i^j) \tag{13}$$

$$\dot{y}_i = n(\mu - r_i^2)y_i + \omega_i x_i + R_y(\phi_i^j) \tag{14}$$

$$R_x(\phi_i^j) = \sum_{j \neq i} (x_j \cos\phi_i^j - y_j \sin\phi_i^j) \tag{15}$$

$$R_y(\phi_i^j) = \sum_{j \neq i} (y_j \sin\phi_i^j + x_j \cos\phi_i^j) \tag{16}$$

where i and j =1,2,3,4 represent the index of each oscillator. ϕ_i^j denotes the phase difference between the i th and the j th oscillator. Quadruped gaits are classified by interlimb coordination, i.e. relative phases between every two limbs. In our model, desired gait can be achieved by specifying the phase difference.

Typical gaits of quadruped locomotion include walk and trot gait. Walk gait has at least three legs touching the ground in a period. Diagonal legs of quadruped robots always move in synchrony during trot gait. Fig. 7 shows the structure of the CPG network and resulting signals for walk and trot gait. The variable x_i is calculated as angular position command of the hip joint of corresponding leg. During locomotion, the knee joint is designed to bend during swing phases and keep motionless during stance phases. Its control signals are given as

$$k_i = \begin{cases} y_i & , \ y_i \le 0 \\ 0 & , \ y_i > 0 \end{cases} \tag{17}$$

where k_i is the angular position command of the knee joint.

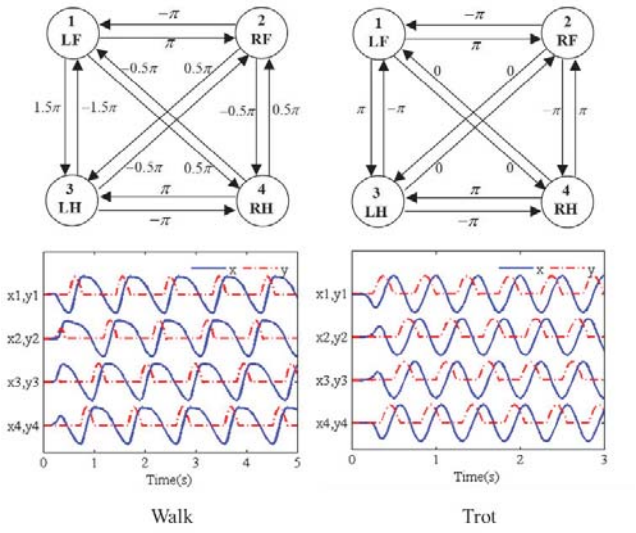

Fig. 6. Coupling structure of the CPG and control signals for the walk gait and the trot gait. Limb 1,2,3,4 represent the left fore limb (LF), the right fore limb (RF), the left hind limb (LH), the right hind limb (RH), respectively. The relative phases for two gaits are labeled on arrows.

V. Experiments and Results

In order to validate the performance of Biodog II, we test walk gait and trot gait over a flat ground surface on our robot. The Hopf oscillator-based CPG is used to generate locomotion trajectories for active joints. The pitch, roll and yaw angles during locomotion are detected to verify the locomotion stability of Biodog II.

A. Walking test

Biodog II is able to walk smoothly and stably at 0.1 m/s – about 0.25 body length per second. Fig. 7 depicts representative images extracted from the video of the walk gait test. The operating sequence of swinging legs in walk gait is RH-RF-LH-LF. It can be seen that all legs in swing phase can lift off the ground and all legs in stance phase can stay in contact with the ground. The pitch, roll and yaw angles detected during walk test are illustrated in Fig. 9 (a). These body angles are all in the range of [-4 4] degrees and fluctuate regularly during walking test.

B. Trotting test

Biodog II locomotes faster with the trot gait than the walk gait at 0.16 m/s – about 0.4 body length per second. Fig. 8 shows snapshots of the trotting test. The operating sequence of swinging legs in trot gait is RF, RH-LH, LF. Diagonal legs move in pairs during trot gait. In Fig. 9(b), the pitch, roll and yaw angles are all in the range of [-5 5] degrees during the trot gait.

From above we can draw a conclusion that the robot Biodog II successfully perform smooth and stable locomotion during both the walk and trot gait.

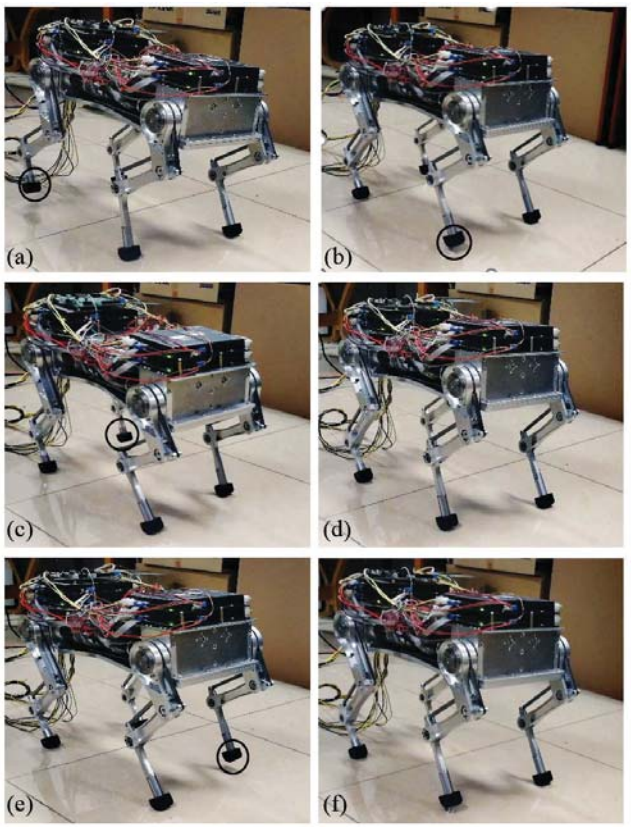

Fig. 7. Snapshots of the walk gait test on Biodog II. The black circles indicate swing limbs. The robot has at least three legs touching the ground in a period: (a) RH lifts up. (b) RF lifts up. (c) LH lifts up. (d) LH touches down. (e) LF lifts up. (f) LF touches down.

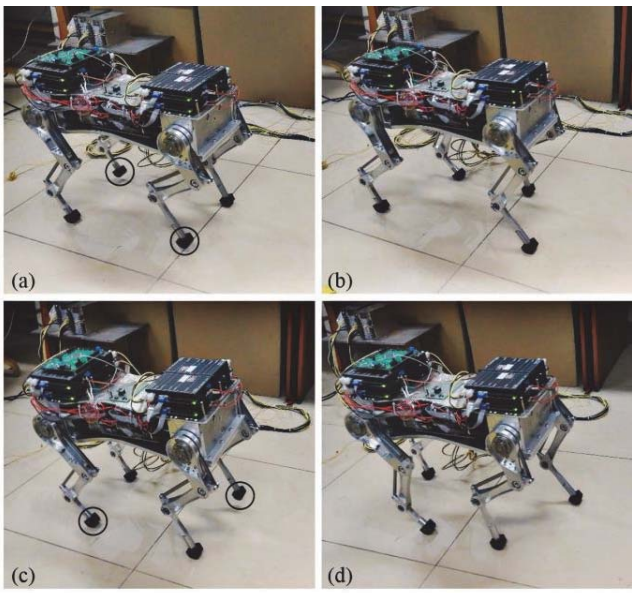

Fig. 8. Snapshots of the trot gait test on Biodog II. The black circles indicate swing limbs. Diagonal legs of the robot move in synchrony: (a) RF and LH lifts up. (b) RF and LH touches down. (c) LF and RH lifts up. (d) LF and RH touches down.

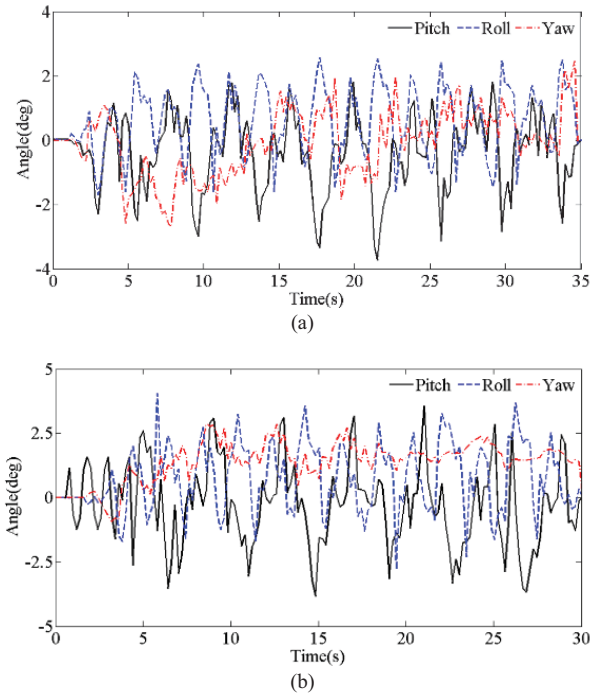

Fig. 9. (a) The pitch, roll and yaw angles of the quadruped robot in walk gait. (b) The pitch, roll and yaw angles of the quadruped robot in trot gait.

VI. Conclusion and Future Work

This paper presents mechanical design and gait control of a novel quadruped robot, "Biodog II", as well as its forward kinematics model and inverse kinematics model. We show how inspiration from biology theory could motivate development of a quadruped robot in terms of design and control. Biodog II features three-segment low-inertia legs and coaxial transmission. We place all DC motors proximal and employ coaxial transmission to achieve efficient fore transmission from motors to active joints. Biodog II employs a tendon-bone co-location architecture, inspired by musculoskeletal structures, to enhance leg strength. Motion trajectories for different gaits are designed by a Hopf oscillator-based CPG. Locomotion control of Biodog II has been implemented using an embedded controller based on an ARM board. The robot Biodog II performs smooth walk and trot gait successfully during experiments, where stability is validated.

Future work will be aimed at equipping Biodog II with more sensors such as a camera and a laser range sensor for practical application. Furthermore, we will supply power to Biodog II with a battery to make the robot self-contained.

References

[1] Toshiba develops tetrapod robot for Tokyo Electric Power Plant Fukushima No.1 Nuclear Power Plant [EB/OL]. http://www.toshia.co.jp/about/press/2012_11/pr2101.htm, 2012.

[2] M. Hutter, C. Gehring and A. Lauber et al, "ANYmal - toward legged robots for harsh environments," *Advanced Robotics*, 2017:1-14.

[3] M. Raibert, K. Blankespoor, G. Nelson, R. Playter, and the BigDog Team, "BigDog, the rough-terrain quadruped robot," *in 17th World Congress on the International Federation of Automatic Control,* pp. 10822-10825, 2008.

[4] C. Semini, N. G. Tsagarakis, E. Guglielmino, M. Focchi, F. Cannella, and D. G. Caldwell, "Design of HyQ – a hydraulically and electrically actuated quadruped robot," *Proceedings of the Institution of Mechanical Engineers, Part I: Journal of Systems and Control Engineering,* vol. 225, no. 6, pp. 831–849, 2011.

[5] C. Semini, V. Barasuol, J. Goldsmith, M. Frigerio, M. Focchi, Y. Gao, and D. G. Caldwell, "Design of the hydraulically-actuated torque-controlled quadruped robot HyQ2Max," *IEEE/ASME Transactions on Mechatronics*, 2016.

[6] M. Hutter, C. D. Remy, M. A. Hoepflinger, R. Siegwart, "Scarl*ETH*: Design and control of a planar running robot," *IEEE/RSJ International Conference on Intelligent Robots and Systems*, pp. 562-567, 2011.

[7] S. Seok, A. Wang, M. Y. M. Chuah, D. J. Hyun, J. Lee, D. M. Otten, J. H. Lang, S. Kim, "Design principles for energy-efficient legged locomotion and implementation on the MIT Cheetah robot", *Mechatronics IEEE/ASME Transactions on*, vol. 20, no. 3, pp. 1117-1129, 2015.

[8] A. Ananthanarayanan, M. Azadi, and S. Kim, "Towards a bio-inspired leg design for high-speed running," *Bioinspiration Biomimetics*, vol. 7, no. 4, pp. 1-12, 2012.

[9] H.-W. Park, P. M. Wensing, and S. Kim, "High-speed bounding with the MIT Cheetah 2: Control design and experiments," *Int. Journal of Robotics Research*, vol. 36, no. 2, pp. 167–192, 2017.

[10] G. Bledt, M. J. Powell, B. Katz, J. D. Carlo, P. M. Wensing, and S. Kim, "MIT Cheetah 3: Design and Control of a Robust, Dynamic Quadruped Robot," in *IEEE/RSJ International Conference on Intelligent Robots and Systems*, pp. 2245-2252, 2018.

[11] G. Kenneally, A. De, and D. Koditschek, "Design principles for afamily of direct-drive legged robots," *IEEE Robotics and Automation Letters*, vol. 1, no. 2, pp. 900–907, 2016.

[12] X. Li, W. Wang, and J. Yi, "Ground substrate classification for adaptive quadruped locomotion," *Proc. Of IEEE International Conference on Robotics and Automation*, 2017.

[13] M. MacKay-Lyons, "Central pattern generation of locomotion: a review of the evidence," *Physical Therapy*, vol. 82, no. 1, pp. 69-83, January, 2002.

[14] A. J. Ijspeert, "Central pattern generators for locomotion control in animals and robots: a review," *Neural Networks*, vol. 21, no. 4, pp. 642–653, 2008.

[15] M. Fischer and R. Blickhan, "The tri-segmented limbs of therian mammals: kinematics, dynamics, and self-stabilization–a review," *Journal of Experimental Zoology. Part A, Comparative Experimental Biology*, vol. 305, pp. 935–952, Nov. 2006.

[16] M. Schmidt and M. Fischer, "Morphological integration in mammalian limb proportions: Dissociation between function and development," *Evolution*, vol. 63, no. 3, pp. 749–766, 2009.

[17] K. Rudman, R. Aspden, and J. Meakin, "Compression or tension? the stress distribution in the proximal femur," *BioMedical Engineering OnLine*, vol. 5, no. 1, p. 12, 2006.

[18] D. R. Carter and W. C. Hayes, "Bone compressive strength: the influence of density and strain rate," *Science*, vol. 194, no. 4270, pp. 1164-1176, 1976.

[19] Yam Geva and Amir Shapiro, "A novel design of a quadruped robot for research purposes," *International Journal of Advanced Robotic Systems*, 2014.

[20] J. Denavit and R. S. Hartenberg, "A kinematic notation for lower-pair mechanisms based on matrices," *ASME Journal of Applied Mechanics*,vol. 23, pp. 215–221, 1955.

[21] L. Righetti, and A. J. Ijspeert, "Pattern generators with sensory feedback for the control of quadruped locomotion," *in IEEE International Conference on Robotics and Automation*, pp. 819-824, 2008.